

Using acoustic emission to understand fatigue crack growth within a single load cycle

Pascoe, J. A.; Zarouchas, D. S.; Alderliesten, R. C.; Benedictus, R.

DOI

[10.1016/j.engfracmech.2018.03.012](https://doi.org/10.1016/j.engfracmech.2018.03.012)

Publication date

2018

Document Version

Final published version

Published in

Engineering Fracture Mechanics

Citation (APA)

Pascoe, J. A., Zarouchas, D. S., Alderliesten, R. C., & Benedictus, R. (2018). Using acoustic emission to understand fatigue crack growth within a single load cycle. *Engineering Fracture Mechanics*, 194, 281-300. <https://doi.org/10.1016/j.engfracmech.2018.03.012>

Important note

To cite this publication, please use the final published version (if applicable). Please check the document version above.

Copyright

Other than for strictly personal use, it is not permitted to download, forward or distribute the text or part of it, without the consent of the author(s) and/or copyright holder(s), unless the work is under an open content license such as Creative Commons.

Takedown policy

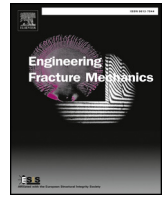
Please contact us and provide details if you believe this document breaches copyrights. We will remove access to the work immediately and investigate your claim.

Green Open Access added to TU Delft Institutional Repository

'You share, we take care!' – Taverne project

<https://www.openaccess.nl/en/you-share-we-take-care>

Otherwise as indicated in the copyright section: the publisher is the copyright holder of this work and the author uses the Dutch legislation to make this work public.



Using acoustic emission to understand fatigue crack growth within a single load cycle

J.A. Pascoe*, D.S. Zarouchas, R.C. Alderliesten, R. Benedictus

Structural Integrity & Composites Group, Faculty of Aerospace Engineering, Delft University of Technology, P.O. Box 5058, 2600 GB Delft, The Netherlands

ARTICLE INFO

Keywords:

Crack growth
Acoustic emission
Fatigue
Adhesive bonding

ABSTRACT

Current methods for prediction of fatigue crack growth are based on empirical correlations which do not take the crack growth behaviour within a single cycle into account. To improve these prediction methods, more understanding of the physical mechanisms of crack growth is required. In this research the acoustic emission technique was used to investigate the crack growth behaviour during a single fatigue cycle. It was found that crack growth can potentially occur both during loading and unloading, but only while the strain energy release rate is above a crack growth (CG) threshold value. The results suggest this CG threshold value is the same in both quasi-static and fatigue loading. Further work is necessary to fully understand the link between the received acoustic emission signals and the actual crack growth processes. Nevertheless, the paper shows the potential of acoustic emission to provide more insight into the physics of crack growth.

1. Introduction

In 1961 Paris and co-workers first introduced the idea that the stress intensity factor (SIF, K) could be used as a similitude parameter to describe fatigue crack growth (FCG) in metals [1]. Although this was considered quite a radical idea at first, it was soon found that the fatigue crack growth rate could indeed be correlated to the SIF range, ΔK , by means of a power-law [2,3]. This relationship has formed the basis for FCG predictions ever since.

Paris' relationship was not only found to work for metals, but was also adopted for fatigue delamination and crack growth in fibre-reinforced polymers (FRPs) and adhesive bonds [4,5]. As the SIF is difficult to compute in layered materials, Irwin's relationship [6] was used to replace K by G , the strain energy release rate (SERR). Other than this substitution, the relationships have the same form as those developed for metals: an empirical power-law correlation between a fracture mechanics parameter (i.e. K or G) and the crack growth rate da/dN . Although models of this form can produce satisfactory predictions of crack growth for engineering purposes, from a scientific point of view they are somewhat unsatisfying.

The empirical nature of these FCG models means there is no physical theory explaining the link between the applied load and the crack growth. For example, no satisfactory explanation has so far been given as to why a power-law relationship between ΔK or G and da/dN should be expected. In the literature, only a few micro-mechanical models could be found that are applicable to crack growth in an adhesive or delamination of a composite [7–10] and of those, only [10] covers fatigue loading.

One reason for this lack of models for the micro-mechanics of fatigue crack growth is that there is little understanding of how the fatigue crack evolves over the course of a single load cycle. Generally a single parameter, e.g. G_{\max} or $\Delta G = G_{\max} - G_{\min}$, is assumed to

* Corresponding author.

E-mail addresses: j.a.pascoe@tudelft.nl, j.pascoe@imperial.ac.uk (J.A. Pascoe).

Nomenclature		<i>t</i>	time (s)
<i>a</i>	crack length (mm)	<i>w</i>	width (mm)
<i>d</i>	displacement (mm)	<i>Subscripts</i>	
<i>G</i>	strain energy release rate (mJ/mm ² , N/mm)		
ΔG	strain energy release rate range (mJ/mm ² , N/mm)	<i>c</i>	critical
<i>K</i>	stress intensity factor (MPa $\sqrt{\text{mm}}$)	<i>I</i>	mode I
ΔK	stress intensity factor range (MPa $\sqrt{\text{mm}}$)	<i>min</i>	minimum
<i>N</i>	cycle number	<i>max</i>	maximum
<i>P</i>	force (N)	<i>th</i>	threshold
<i>R</i>	load ratio		

be representative for the crack driving force during an entire cycle. Similarly, a single value of da/dN is assumed to be representative for the crack growth rate during an entire cycle. This means that either da/dN is interpreted as an average value, or that the crack growth rate is (implicitly) assumed to be constant during the entire load cycle.

As during a fatigue cycle the imposed load is constantly changing, it would seem logical that the crack growth rate is also not constant. It may also be the case that the crack only grows during certain portions of the load cycle, e.g. only when the load is above a certain value, or only during the loading phase. For the purposes of engineering predictions, it may be sufficient to neglect this. However, from a scientific standpoint a full description of the crack growth process is desirable. Such an understanding could help resolve outstanding questions, such as how to deal with the *R*-ratio effect which has been reported for fatigue crack growth in adhesives and composites [11–14].

The existence of the *R*-ratio effect implies that it is not possible to describe a fatigue cycle by just one parameter; more information about the fatigue cycle needs to be taken into account. The question then becomes, which information? Thus the research presented in this paper aimed to identify experimentally during which portions of the load cycle crack growth occurs, as a step towards identifying which aspects of the fatigue cycle are relevant for crack growth. This will hopefully lead to a more fundamental description of the relationship between the applied load and fatigue crack growth.

In order to determine during which part of the cycle crack growth occurred, the acoustic emission (AE) technique was used. This technique is based on the research of Kaiser [15] and works by using one or more piezoelectric transducers to measure the ultrasonic sound-waves produced when crack growth occurs. This allows the detection of the occurrence of crack growth, even if the crack growth increment is too small to be detected visually. It was hypothesised that by measuring the time at which signals are detected and comparing this with the applied load, it is possible to determine during what portion of the load cycle fatigue crack growth actually occurs.

AE is under active investigation as a means of locating damage and measuring damage size in composite or adhesively bonded materials, as e.g. recently reported in [16–19]. It should be stressed that this was not the purpose of the current research. The question was not *where* damage occurred, but *when* it occurred, within a single cycle. In other words, the question this research addresses is: should the entire load cycle be taken into account to describe the fatigue crack driving force, or only a portion of the cycle? If only a portion is important, which portion?

This paper presents a proof-of-concept of using AE to investigate this question experimentally, as well as discussing some results that can be used to inform the development of more physically correct models for crack growth. Some similar work has been done in this area previously [20,21], but focussing on damage in FRPs. Additionally only [20] attempted to identify during which portion of the cycle crack growth occurred.

The contents of this paper is as follows: Section 2 discusses why it is necessary to gain more understanding of the fatigue crack behaviour within a single cycle. Section 3 describes the test set-up and the applied loads. In order to build up towards understanding crack growth under fatigue loading, first crack growth was examined under quasi-static loading, followed by fatigue loading with a low displacement rate (1 mm/min). The final stage of the experiments involved fatigue load cycles with a frequency of 5 Hz. Section 4 presents the results of the quasi-static loading, and Section 5 discusses the fatigue experiments. The conclusions are summarised in Section 6.

2. Need for an understanding of FCG behaviour within a single cycle

Since the work of Roderick et al. [4], and Mostovoy and Ripling [5], the models that have been proposed for FCG in FRPs or adhesive bonds are generally of the form:

$$\frac{da}{dN} = Cf(G)^n \tag{1}$$

where *C* and *n* are empirical parameters determined by curve-fitting, and *f*(*G*) is some function of *G*; generally *G*_{max} or ΔG . Various modifications are then introduced in order to account for effects such as *R*-ratio or mode-mixety, but the underlying form is always the same [22].

The Paris equation was originally introduced as being based on the stress at the crack tip. While the Irwin equivalence means that *G* can also be understood as being representative for the crack-tip stress, it is fundamentally an *energy* parameter. Thus it makes sense

to examine Eq. (1) in light of the Griffith energy balance concept [23], which states that the amount of strain energy released during (stable) crack growth must equal the amount of energy required to create new fracture surfaces. This approach raises some interesting questions regarding the physical meaning of Eq. (1).

Let us consider first of all the case where $f(G) = G_{\max}$, i.e. the G at maximum load. G is defined as the amount of strain energy released per increment of crack growth. G depends on the geometry, the force, and the displacement. As such, it continuously changes during the load cycle. I.e. an increment of crack growth occurring at maximum load will release a different amount of energy than an increment occurring at some other point in the fatigue cycle.

The Griffith energy balance principle requires that the crack growth should be proportional to the total amount of energy released during a fatigue cycle. This principle was used by Weertman to formulate a fatigue crack growth model [24,25] based on the amount of energy released during a cycle. The energy approach has been further developed by Chudnovsky and Moet [26,27], and Ranganathan et al. [28,29]. In a somewhat similar approach, Meneghetti et al. [30,31] have related the fatigue strength to the amount of heat dissipated during a fatigue cycle. The relationship between crack growth rate and energy dissipation has also been experimentally studied in an epoxy adhesive [32] and a carbon-fibre reinforced polymer (CFRP) [33,34].

From the research mentioned above, it is clear that fatigue crack growth depends on energy dissipated over the course of a fatigue cycle. However, this is not reflected in common crack growth models. For example, using G_{\max} in Eq. (1) implies that only the energy released by a crack growth increment occurring at maximum load is of importance for fatigue crack growth. Unless fatigue crack growth only occurs at the maximum of the load cycle, it seems logical that the energy release at other points during the cycle should also be taken into account.

This can also be seen by the existence of the R -ratio effect. One can create an infinite number of different load cycles that all have the same G_{\max} , but a different R -ratio, as illustrated in Fig. 1. If only G_{\max} determines the crack growth rate, then all these load cycles should produce the same amount of crack growth. It is well established that this is not the case in practice however; different R -ratios will produce different crack growth rates. Thus it appears that G_{\max} alone cannot be used to accurately predict the crack growth rate, and that the G values at other points in the cycle need to be taken into account.

Similar objections apply to the use of ΔG . One can create an infinite number of fatigue cycles with identical ΔG , but different R -ratios (see Fig. 2), and again it will be seen that the crack growth rate will be different for different R -ratios. As ΔG is defined as $G_{\max} - G_{\min}$, ΔG in principle takes two points of the fatigue cycle into account. However, by subtracting G_{\max} and G_{\min} only the distance between these two points is taken into account, and not the absolute values. As G is defined as the amount of energy that is released by an increment of crack growth, it would seem logical that the absolute value of the energy released is important, and not just the difference between the maximum and minimum value.

Furthermore, one can ask, what is the physical meaning of G_{\min} ? Following the definition of G , G_{\min} is the amount of strain energy released by an increment of crack growth occurring at minimum load. But is there in fact crack growth at minimum load? If there is, why does the crack not grow if fatigue cycling is stopped, and the load is held constant at the minimum level? If G_{\min} is sufficiently high there may be creep, but if G_{\min} is close to 0, no crack growth will occur. If there is no crack growth, and thus no energy release, at minimum load, then what is the physical meaning of G_{\min} , and why should the crack growth depend on $G_{\max} - G_{\min}$?

More generally, one can pose the question: If a single parameter is insufficient to uniquely describe a fatigue load cycle, then why would a single parameter be sufficient to uniquely describe the resulting crack growth rate?

Since two parameters are required to define a load cycle, a number of researchers have proposed methods that attempt to correlate the crack growth rate to (at least) two variables; generally either G_{\max} and ΔG , or G_{\max} and R . Examples include: [11,13,14,35–37]. These methods are still based on empirical correlations however [22], rather than on an understanding of the underlying physics. Furthermore, the forms of the equations given in the mentioned papers implicitly carry with them an assumption

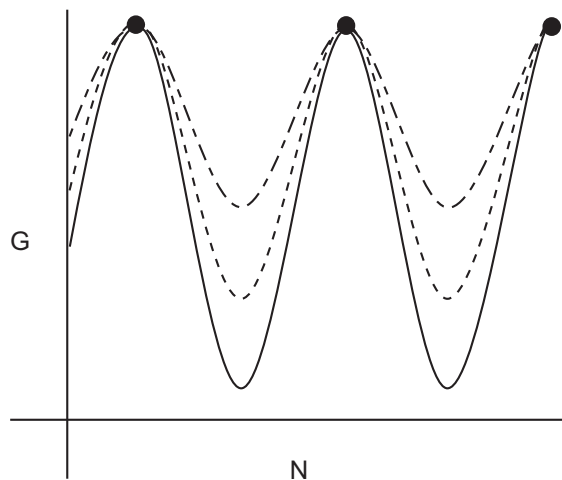


Fig. 1. There are an infinite number of possible fatigue cycles with the same G_{\max} . Each will result in a different FCG rate. Thus G_{\max} alone is not sufficient to describe FCG.

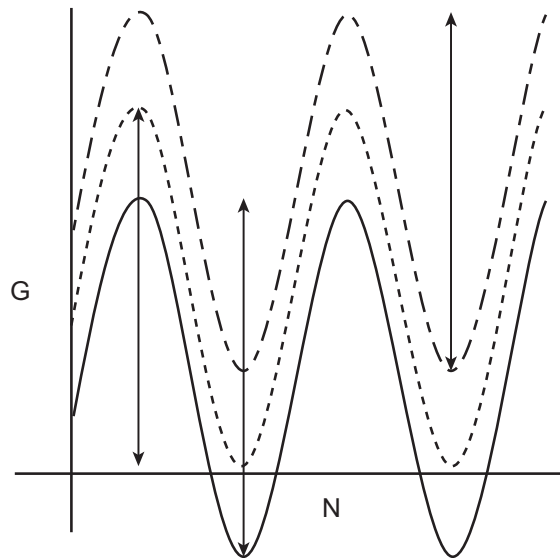


Fig. 2. There are an infinite number of possible fatigue cycles with the same ΔG . Each will result in a different FCG rate. Thus ΔG alone is not sufficient to describe FCG.

of which portion of the fatigue cycle is important. Thus it seems valuable to make this aspect explicit, and to first determine which portion of the fatigue cycle is actually important in practice, so that future models can be developed on this basis.

To understand which portion of the fatigue cycle is important for crack growth, it is first necessary to understand how the FCG behaviour changes over the course of a fatigue cycle. Does crack growth only occur at maximum load, or also at other points during the cycle? Does growth occur during the loading or unloading portion of the cycle, or during both portions? If the latter, is there any difference between growth during the loading portion and during the unloading portion? Does the absolute magnitude of the SERR matter, or only its value relative to the minimum SERR? These are the questions that the current research set out to answer.

3. Test set-up

This section describes the specimens used in the experimental part of this work, as well as the acoustic emission equipment and settings, and the test programme.

3.1. Specimens

The specimens used in this test were double cantilever beam (DCB) specimens, consisting of two aluminium Al2024-T3 arms with a nominal thickness of 6 mm, bonded with Cytec FM-94 epoxy adhesive. Specimen manufacturing started with two aluminium plates, which were pretreated with chromic acid anodisation (CAA) and an application of BR-127 primer. A layer of FM-94 film with a polyester carrier was placed between the plates. This stack was then cured in an autoclave at a pressure of 0.4 MPa and a temperature of 120 °C for 1 h, in accordance with the adhesive manufacturer's specifications. After curing the plate was cut into strips, which were then milled down to the final dimensions. Threaded holes were drilled into the specimens, in order to be able to bolt on loading blocks to connect the specimens to the loading machine. The final nominal specimen dimensions were a width of 25 mm and a length of 300 mm.

Prior to the adhesive bonding a thin Teflon film was placed along one edge of the aluminium plates in order to create in the final specimens a pre-crack with a length of approximately 30 mm (measured from the load application point). More details on the manufacturing process can be found in [38], and the actual measured specimen dimensions are available in the online dataset [39].

Before testing, the edges of the specimens were coated with thinned type-writer correction fluid in order to enhance visibility of the crack-tip. This is a standard procedure for crack growth tests, but as will be discussed in Section 4.2 it may have caused issues with the crack length measurement in this case.

Three specimens were produced for this experiment, denoted AE-001, AE-002, AE-003. Valid data was obtained for the experiments on AE-001 and AE-003. For specimen AE-002 failure of the thread of the lower bolt holes occurred before any crack growth was detected. The bolt thread failed at an applied force of approximately 2.1 kN; more than a factor of 2 higher than the maximum force needed to cause crack growth in the other specimens. The most likely hypothesis to explain this result is that for specimen AE-002 the film insert did not act as a crack-starter as intended. This was not verified further however.

3.2. Acoustic emission

An AMSY-6 Vallen, 8-channel acoustic emission system with 4 parametric input channels was used in order to perform the AE measurements. One wide-band piezoelectric sensor, AE1045S, with an external 34 dB pre-amplifier and a band-pass filter of 20–1200 kHz, was clamped on the specimens as illustrated in Fig. 3. Grease was applied on the surface of the specimen so as to increase the conductivity between the sensor and the specimen. In order to ensure the conductivity, pencil break tests were conducted before each experiment. This involves pushing the lead of a mechanical pencil against the specimen until the pencil lead breaks and then confirming that the resulting acoustic emission is detected by the system. Two parametric input channels were used to monitor the force and displacement and correlate them to the AE data. The parametric data sets were generated at a predefined time interval which was 1 s for the quasi-static tests and 0.01 s for the fatigue tests.

3.3. Selection of the acoustic emission threshold

In order to filter out noise, the AE system does not record signals for which the peak amplitude does not exceed a pre-defined threshold. In this research there are therefore two types of threshold, which should not be confused. One is the minimum AE signal amplitude that is recorded. This will be referred to as the AE threshold. The other is the (hypothetical) load level below which there is no crack growth, which shall be referred to as the crack growth (CG) threshold.

Correct selection of the AE threshold is an important experimental consideration. Setting the AE threshold too low will result in recording noise, in addition to the signals generated by crack growth. This makes post-signal analysis needlessly time-consuming. On the other hand, if the AE threshold value is too high, then valid AE signals will not be recorded.

Based on prior experience, an AE threshold value of 62 dB was selected for the tests on specimen AE-001. During the tests on specimen AE-003, it was investigated whether a lower AE threshold setting could be used. First a setting of 50 dB was tried. This resulted in detection of an AE signal at a very low load level, corresponding to $G \approx 0.01$ N/mm. A closer analysis of this signal indicated it was most likely noise. Therefore the AE threshold was raised to 55 dB, and that value was used for all further tests on AE-003. The effect of the difference in AE threshold between the tests on AE-001 and AE-003 was analysed and will be discussed together with the other test results.

3.4. Selection of parameters to study

When acoustic emission signals are recorded, a number of different parameters can be investigated. For example, one can look at the peak amplitude of the signal, the rise time, or the energy content. Instead of just looking at a single signal, one can also e.g. investigate the cumulative received energy instead. Therefore, it is necessary to justify why the peak amplitude was selected for investigation in this research.

As the objective of this research was to identify at which points during a fatigue cycle crack growth can take place, it seemed more appropriate to look at the characteristics of individual signals, rather than at cumulative parameters. Crack growth is known to involve the sudden release of strain energy, thus it seemed logical to investigate the amplitude of the signals. As the peak amplitude and energy per event are strongly correlated, only the peak amplitude is presented in this paper, in order to conserve space. To facilitate further analysis, the recorded energy per event has been included in the online dataset accompanying this paper [39].

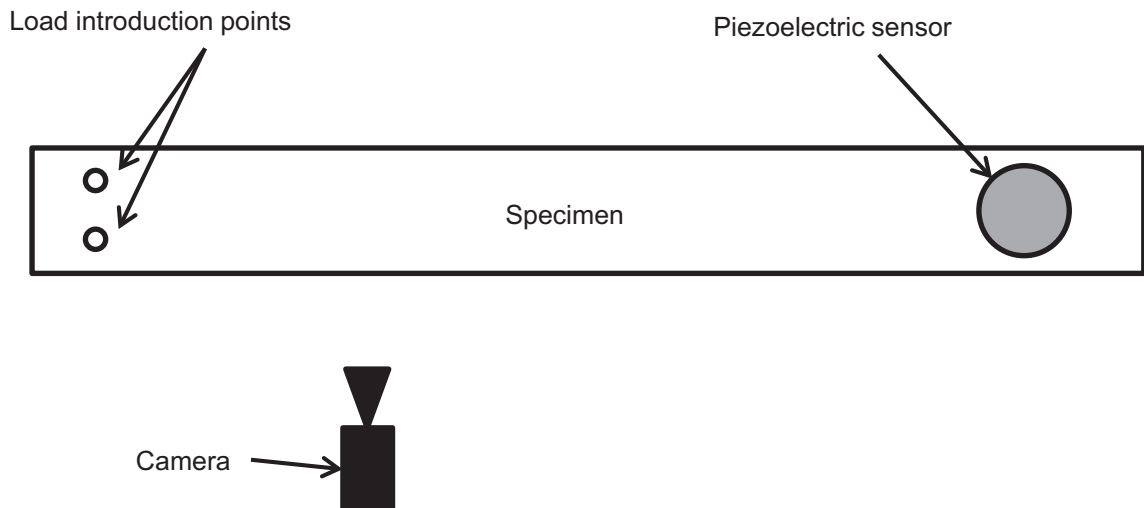


Fig. 3. Schematic illustration of the test set-up, showing a top-view of the specimen and the placement of the piezoelectric sensor and the camera. The load was applied normal to the plane of the illustration. The figure is not to scale.

3.5. Test programme

All tests were performed under displacement control on an MTS 10kN servo-hydraulic fatigue machine. Crack length was monitored by means of a camera aimed at the side of the specimen. As the camera position was not exactly the same for each experiment, the precise resolution varied on the order of 15–22 pixels/mm. Force and displacement were measured by the fatigue bench. At the most recent calibration the accuracy of this force measurement was determined to be 0.64% at 100 N and 0.18% at 1 kN. The accuracy of the displacement measurement was determined to be 0.12% at 1 mm and 0.08% at 10 mm.

The force and displacement measurements were output to the computer controlling the crack growth camera and to the AE system. This allowed crack length measurements and AE signal detections to be synchronised with the corresponding force and displacement values. The test set-up is shown schematically in Fig. 3.

The SERR was computed according to the equation for a DCB specimen, as given in ASTM standard D 5528 [40]:

$$G = \frac{3Pd}{2wa} \quad (2)$$

where P is the force, d is the displacement, w is the width of the specimen and a is the crack length. It is well-known that this equation underestimates the true SERR value [40]. However, as the objective of this research was to compare the behaviour between the different tests, rather than generate accurate material data, the simplicity of this method was deemed to outweigh the reduced accuracy.

A number of different load cases were applied, in order to investigate different aspects of crack growth behaviour. First crack growth under quasi-static loading was investigated, then the effect of load cycles with a very low rate (1 mm/min displacement) and finally fatigue load cycles with a frequency of 5 Hz. Results will be presented for the following load cases:

- Quasi-static (QS) loading at 1 mm/min until first AE signal detection, then holding the displacement.
- QS loading at 1 mm/min until the force drops again, then holding the displacement.
- Fatigue cycles at a 1 mm/min displacement rate with $R = 0$.
- Fatigue cycles at a 1 mm/min displacement rate with $R = 0.5$.
- Fatigue cycles at 5 Hz with varying R ratios.

The load cases allow a comparison between fatigue crack growth behaviour under quasi-static and fatigue loading. They also allow investigation of the question whether crack growth only occurs when the test machine is in motion, or whether it can also occur for constant load, which might explain some frequency effects. A full overview of the different experiments and which load case was applied is given in Table 1.

Table 1

Test matrix, listing the different experiments and the applied load cases. The raw data for each experiment is available from [39]

Experiment	Load case
AE001-QS1	QS load at 1 mm/min until the first acoustic emission signal, then displacement held constant
AE001-QS2	QS load at 1 mm/min until drop in the force. Fatigue machine safety interlock activated before this happened. Therefore the collected data will not be discussed in this paper. Higher capacity load cell (10 kN) installed after this test
AE001-QS3	QS load at 1 mm/min until drop in the force, then displacement held constant
AE001-QS4	QS load at 1 mm/min until crack length had been extended to roughly 100 mm
AE001-QS5	QS load at 1 mm/min until drop in the force, then displacement held constant
AE001-Fat1	5 Fatigue cycles at 1 mm/min displacement rate. $d_{max} = 1.39$ mm, $d_{min} = 0$ mm, ($R = 0$)
AE001-Fat2	5 Fatigue cycles at 1 mm/min displacement rate. $d_{max} = 1.39$ mm, $d_{min} = 0$ mm, ($R = 0$)
AE001-Fat3	5 Fatigue cycles at 1 mm/min displacement rate. $d_{max} = 1.39$ mm, $d_{min} = 0$ mm, ($R = 0$)
AE001-Fat4	5 Fatigue cycles at 2 mm/min displacement rate. $d_{max} = 1.39$ mm, $d_{min} = 0$ mm, ($R = 0$)
AE001-Fat5	5 Fatigue cycles at 1 mm/min displacement rate. $d_{max} = 1.39$ mm, $d_{min} = 0.695$ mm, ($R = 0.5$)
AE001-Fat6	Fatigue cycles at 5 Hz. $d_{max} = 1.39$ mm, $d_{min} = 0.695$ mm, ($R = 0.5$). AE system recording frequency set too low, resulting in aliasing, this experiment will not be discussed in this paper
AE001-Fat7	Fatigue cycles at 5 Hz. $d_{max} = 1.39$ mm, $d_{min} = 0.695$ mm, ($R = 0.5$)
AE001-Fat8	5 Fatigue cycles at 1 mm/min displacement rate. $d_{max} = 1.39$ mm, $d_{min} = 0.695$ mm, ($R = 0.5$)
AE001-Fat9	5 Fatigue cycles at 1 mm/min displacement rate. $d_{max} = 7.6$ mm, $d_{min} = 0$ mm, ($R = 0$)
AE001-Fat10	5 Fatigue cycles at 1 mm/min displacement rate. $d_{max} = 7.6$ mm, $d_{min} = 3.8$ mm, ($R = 0.5$)
AE003-QS1	QS load at 1 mm/min in order to create a cohesive crack. Test stopped after onset of crack growth determined visually
AE003-QS2	QS load at 1 mm/min until the first acoustic emission signal. Then displacement held constant. Test repeated with a higher AE threshold. Test repeated again, but only holding after the first cluster of signals, rather than the first hit
AE003-QS3	QS load at 1 mm/min until drop in the load, then displacement held constant
AE003-Fat1	5 Fatigue cycles at 1 mm/min displacement rate. $d_{max} = 2.27$ mm, $d_{min} = 0$ mm, ($R = 0$)
AE003-Fat2	5 Fatigue cycles at 1 mm/min displacement rate. $d_{max} = 2.27$ mm, $d_{min} = 1.135$ mm, ($R = 0.5$)
AE003-Fat3	5 Fatigue cycles at 1 mm/min displacement rate. $d_{max} = 1.9$ mm, $d_{min} = 0$ mm, ($R = 0$)
AE003-Fat4	5 Fatigue cycles at 1 mm/min displacement rate. $d_{max} = 1.9$ mm, $d_{min} = 0.95$ mm, ($R = 0.5$)
AE003-Fat5	Fatigue cycles at 5 Hz. $d_{max} = 2.27$ mm, $d_{min} = 0.95$ mm, ($R = 0.42$)
AE003-Fat6	Fatigue cycles at 5 Hz. $d_{max} = 2.27$ mm, $d_{min} = 0$ mm, ($R = 0$)

For specimen AE-001 a quasi-static load was used to generate a cohesive crack starting from the crack-starter that was placed during manufacturing. No data was collected during this procedure however. For specimen AE-003 data was collected during this procedure, and this was labelled experiment AE003-QS1 (see also Table 1). Apart from experiment AE003-QS1 all experiments started from a sharp cohesive crack.

Both the raw and analysed experimental data is available online [39].

4. Results and discussion - quasi-static loading

Test results were obtained for specimens AE-001 and AE-003. As mentioned above, for specimen AE-002 failure of the thread of the lower bolt holes occurred before any crack growth was detected.

4.1. Quasi-static loading until first emission

In the first load case a quasi-static load was applied at a displacement rate of 1 mm/min. As soon as an acoustic emission event was detected (referred to as a ‘hit’ in this paper) the displacement was held at the value that had been reached at that point, while continuing to record data. The results are shown in Fig. 4.

For specimen AE-001 one test was performed: AE-001-QS1. For this test the AE detection threshold was set to 62 dB. There was a cluster of hits starting just before the maximum load was reached, with more hits later during the hold. The initial cluster of hits is associated with a number of emissions with very high energy content, with later signals only reaching about 1/10th of the maximum energy value recorded during the initial cluster. No crack growth was visible during this test.

For experiment AE003-QS2 the load case was applied three times. During the first load application an AE threshold of 50 dB was used. This resulted in a hit at a very low load level ($G \approx 0.01$ N/mm). Analysis of this signal indicated that this was most likely noise. Thus it was decided to raise the detection limit to 55 dB for the second load application. During this test one small cluster of hits was detected, with a maximum peak amplitude of just under 60 dB. No further hits were detected when the displacement was held. During unloading of the specimen however a new cluster of hits was detected. No crack growth was visible during this second test.

For the third load application it was decided to keep increasing the displacement until a hit was detected with a peak amplitude above 60 dB. In this case there was a ‘baseline’ of signals at around 55 dB that continued for the entire duration that the displacement was held. At irregular intervals there was a signal with a higher amplitude. During unloading there was another cluster of hits. Again the signal associated with the initial loading had the highest energy content, although the difference between the initial and later signals was smaller in this case.

The crack growth during this third test is shown in Fig. 5. There was approximately 0.75 mm of crack growth coincident with the first cluster of hits above 60 dB. During the first minutes of the subsequent hold there was a further crack growth of about 0.2 mm. After this the crack length was constant. The peak force was 483 N. After the displacement was held the force decreased until it reached a constant value of 470 N.

These results suggest that the cluster of hits that occurred during loading is indeed indicative of crack growth. Given the lack of visible crack growth and the constant force (implying constant compliance) from about time $t = 2500$ s onwards, it seems that the

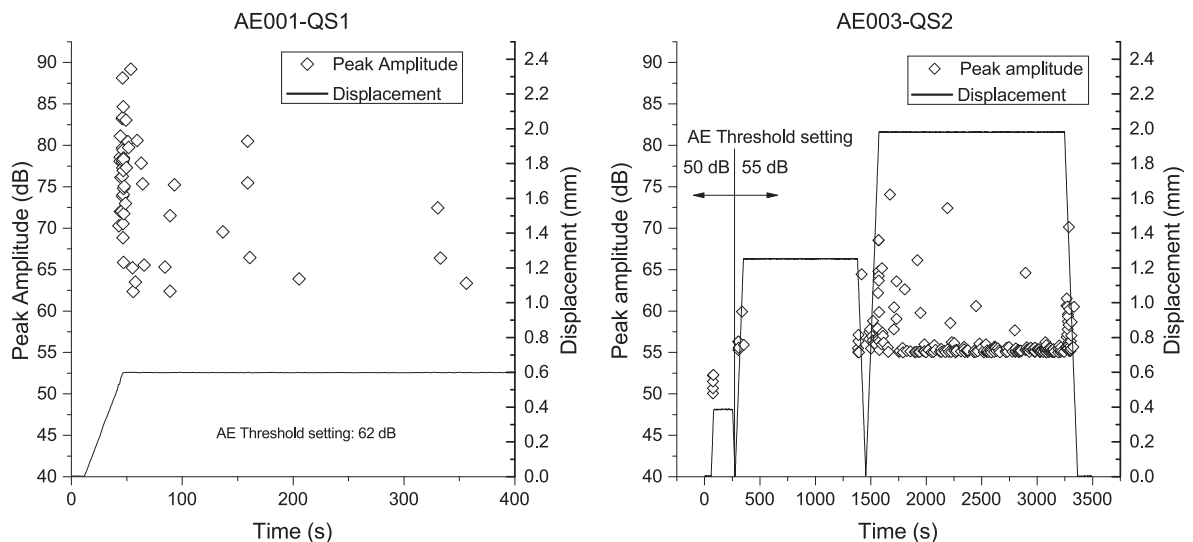


Fig. 4. Displacement and peak amplitude of the received acoustic signals for the load case where the displacement was held as soon as the first signals were detected. This load case was performed once on specimen AE001 (experiment AE001-QS1, left panel) and three times on specimen AE003 (experiment AE003-QS2, right panel). The detection threshold for the acoustic emission system was raised between the first and second test on specimen AE-003, as analysis of the waveform suggested the signals detected during the first test were just noise.

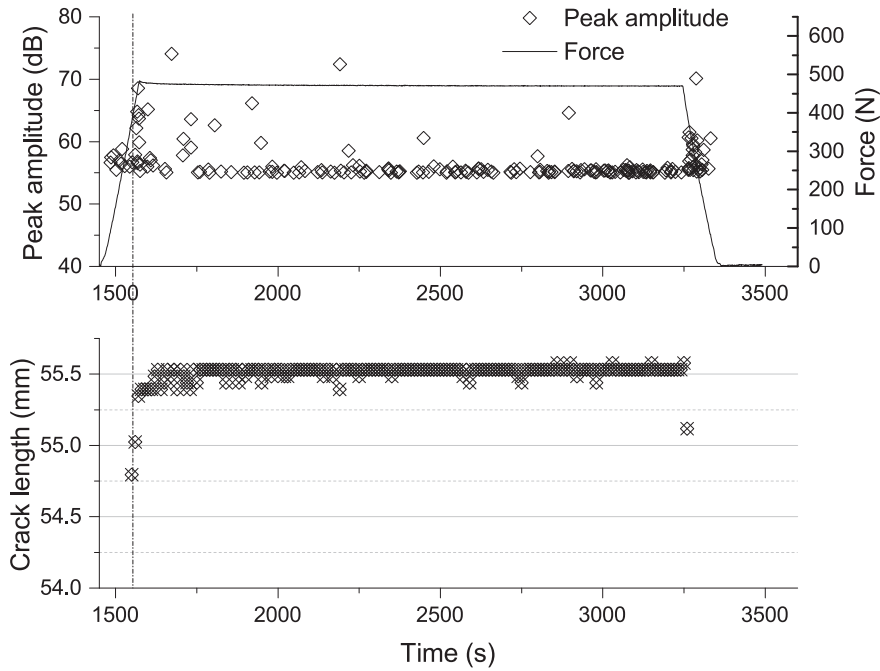


Fig. 5. Force, peak amplitude, and crack growth for the third load application during experiment AE003-QS2. The displacement was held as soon as the first AE signals with an amplitude greater than 60 dB were detected. There was approximately 0.75 mm of crack growth coincident with the first cluster of AE hits above 55 dB, as indicated by the vertical line. During the first minutes of the subsequent hold the crack grew by approximately another 0.2 mm.

55 dB signals are not indicative of crack growth. Given that there was no relaxation of the force required to maintain the constant displacement, visco-elastic effects can also be ruled out.

From the point of view of the energy balance concept [23,41,42] during the initial loading a certain amount of energy is added to the system. Some of this energy is available for crack growth, and is dissipated by the crack growth process. The results shown here suggest that this dissipation is not an instantaneous process but instead occurs over a period of time, while the load is held above some value (though not necessarily held constant). Thus crack growth can continue until the entire ‘packet’ of energy available for crack growth is depleted.

This may also partially explain the frequency effect sometimes seen in fatigue. If crack growth can continue for some period even

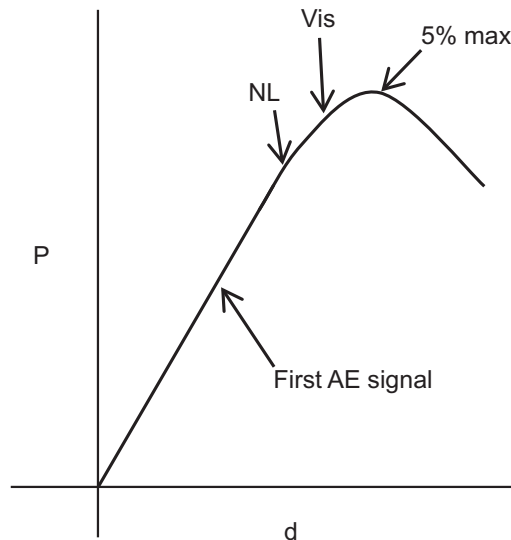


Fig. 6. Schematic illustration of the result that acoustic emission suggests that crack growth occurs for $G < G_{Ic}$. [40] offers 3 means of determining G_{Ic} from the force-displacement curve, combined with observation of the crack growth. I.e: non-linearity of the curve (NL), onset of visual crack growth (VIS), and the 5% offset (5% max). However, during these experiments the first acoustic signals were detected at force and displacement values that correspond to much lower values of G than any of the ASTM values.

with a constant load, it means that it is not only important what maximum load is reached, but also how long a specimen remains at that load. A lower frequency of fatigue loading means that for the same number of cycles, the specimen will have spent a longer time at high load and therefore more crack growth will have occurred.

It should be noted that in this experiment crack growth occurred without any visually apparent non-linearity of the force-displacement curve. This can be seen in Fig. 5. Since the displacement rate was constant, the linearity of the force vs time curve implies linearity of the force-displacement curve. There was also no drop in the load until the displacement was held. Non-linearity of the force-displacement curve and occurrence of a peak load are the events that are used to identify the critical SERR G_{Ic} in the ASTM testing standards [40,43]. In particular, in the ASTM standards G_{Ic} is related to one of three points. Those are: the point where the force-displacement curve becomes non-linear (NL), the point where crack growth is determined visually (VIS) or the intersection of a 5% offset line (5% max). These points are schematically indicated in Fig. 6. As is also indicated in that figure, in the present test the first AE hits were detected well before reaching one of these points, suggesting that crack growth can occur before reaching G_{Ic} .

The choice of AE threshold will affect at which point on the P - d curve of Fig. 6 the first AE signal is detected; as can be seen in Fig. 5 the first AE signals had a slightly lower amplitude than those detected slightly later. Therefore the choice of detection threshold will affect which value of G is identified as the initiation value for crack growth based on AE. Regardless of the precise value of G_I identified in this way however, it will be lower than the G_{Ic} value determined using one of the ASTM definitions. This means that G_{Ic} as defined in the ASTM standards should not be understood as the lowest G value at which crack growth occurs.

4.2. Quasi-static loading until load drop

In the second load case the displacement was increased at a rate of 1 mm/min, until a drop was observed in the recorded force. After the force dropped the displacement was held constant, while continuing to record data. On specimen AE001 this experiment was performed twice, once at a ‘short’ crack length (on the order of 40 mm, test AE001-QS3) and once at a ‘long’ crack length (on the order of 105 mm, test AE001-QS5). The results for specimen AE001 are shown in Fig. 7. In both cases no emissions were detected during initial loading until a certain force/ displacement value was reached. Then there was a cluster with many hits per unit of time, until the displacement was held. After holding the displacement, the number of hits per time decreased, as did the peak amplitude of the signals.

During the loading there was a large amount of crack growth, coincident with the cluster of AE hits. Again this crack growth started before reaching the maximum force, and without causing visually apparent non-linearity of the force-displacement curve. After the displacement was held the crack continued to grow, albeit at a much lower rate. The crack growth rate appeared to reduce over time.

For experiment AE001-QS3 there appears to be a step in the crack length at around $t = 2000$ s. This is most likely an issue with the

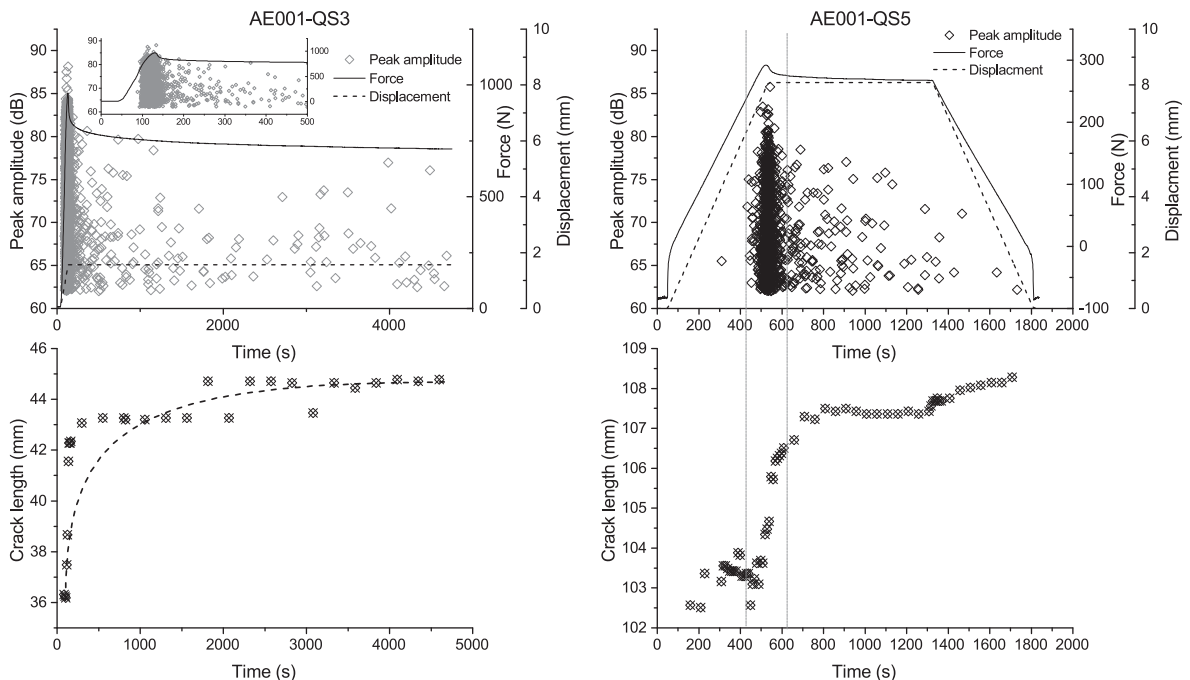


Fig. 7. Crack length, force, and peak amplitude of the acoustic emission signals for experiments AE001-QS3 and AE001-QS5. The load case was 1 mm/min displacement increase until the force decreased, at that point the displacement was held constant. The acoustic emission threshold was set to 62 dB. The dashed line in the bottom left panel is thought to give a more accurate approximation of the crack growth behaviour than the recorded crack length measurements, due to the measurement issues discussed in Fig. 8.

crack length measurements that was encountered in a number of experiments and is illustrated in Fig. 8: there was not always obvious movement of a crack tip. Rather there was a faint line visible in the crack tip photos that gradually became more distinct. This was interpreted as a sudden jump in the crack length when the line was distinct enough. Physically one would not expect a sudden jump in crack length, and certainly not of this magnitude. Furthermore the force vs time curve is smooth, whereas a jump in crack length should produce a corresponding drop in the force (given the constant displacement). Thus the most likely explanation is that in some cases the crack growth in the adhesive was continuous, whereas the crack growth in the paint layer occurred in jumps, either lagging behind, or jumping ahead of the crack growth in the adhesive. For future experiments it is recommended to use a thinner paint layer, and to investigate the possibility of tracking the crack tip without using a paint layer at all.

An additional consideration is that in a DCB test, the crack front is generally curved (see e.g. [44]), implying that the crack growth behaviour at the free edges is not the same as in the bulk material. However, with the available test set-up, only the side of the specimen could be observed. Thus it is also quite possible that the crack growth at the visible edge of the specimen was discontinuous, whilst the crack growth in the bulk material was more continuous.

To better understand how long the crack keeps growing a long duration version of this ‘hold at maximum force’ load case was performed on specimen AE-003. The results of this experiment (AE003-QS3) are shown in Fig. 9. After sudden reduction of the force was observed, the displacement was held constant for about 18.5 h. During this time approximately 1 mm of crack growth was observed. Unfortunately it could not be determined when exactly during the test this crack growth occurred, due to the issues discussed in the previous paragraph and illustrated in Fig. 8. Given the smoothness of the force vs time curve, it seems most likely that the crack growth occurred in a continuous manner as indicated by the dashed line in Fig. 9, and not in the discontinuous fashion suggested by the data points.

There is a continuous ‘baseline’ of low amplitude hits (i.e. 55–58 dB), the maximum peak amplitude of which steadily increases up to about $t = 45,000$ s. The maximum peak amplitude of the signals ‘above’ this baseline shows a decreasing trend over the same period. The source of these baseline signals is unclear. It cannot be excluded that these signals are related to crack growth that could not be visually detected (either due to resolution of the camera or due to the crack growth occurring below the surface of the specimen). However the lack of a reduction in the force during the last portion of the test suggests that no crack growth (or visco-elastic relaxation) occurred there, despite the AE signals.

4.3. Crack growth threshold

For the experiments discussed in this section acoustic emission did not start immediately, but only after a certain load level had been reached. Making the assumption that no crack growth occurs without acoustic emission, this allows the determination of a CG threshold SERR value. However, the question then becomes which detected signals to interpret as indicative of crack growth.

Based on the data from experiment AE003-QS2 (Fig. 4, right panels) it seems that the signals with a peak amplitude < 58 dB, are not correlated to crack growth. It is of course possible that the signals < 58 dB detected during AE003-QS2 were caused by crack growth that was too small to be detected visually, or by crack growth that could not be detected due to it taking place in the centre of the specimen, rather than at the edge. This is an issue that needs further investigation in future. For the remainder of this paper it will be assumed that signals with a peak amplitude < 58 dB do not correspond to crack growth.

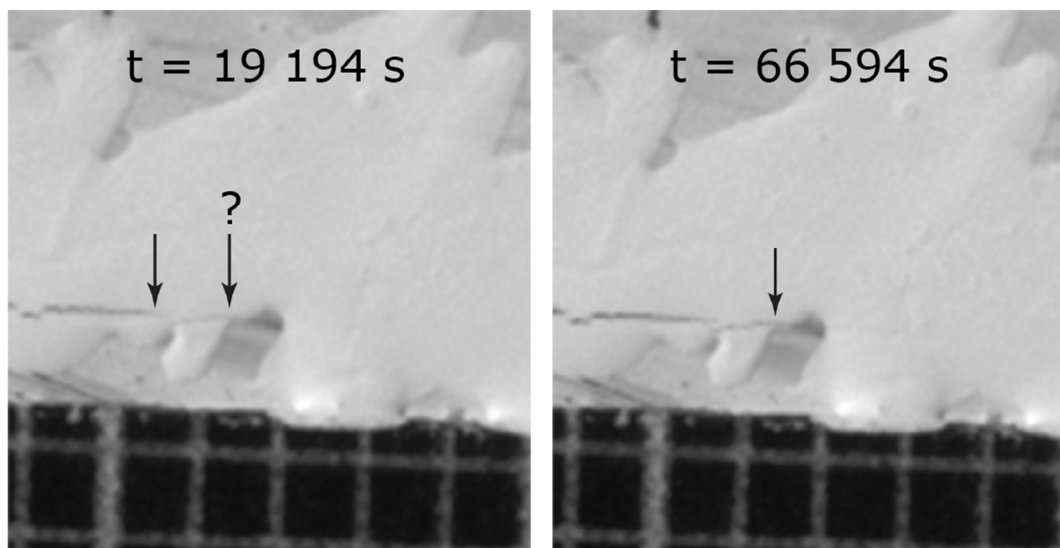


Fig. 8. Example of the issues with crack length measurement. This figure shows a portion of two photos taken during test AE003-QS3. At $t = 66,594$ s the crack tip is located at the arrow. However at $t = 19,194$ s it is not clear whether the left or the right arrow indicates the crack tip. No crack tip advance was obvious. Rather, the faint line between these two arrows gradually became less faint in later pictures. This causes the jump in the crack length measurements as shown in Figs. 7 and 9, even though the actual crack growth was most likely a gradual, continuous process.

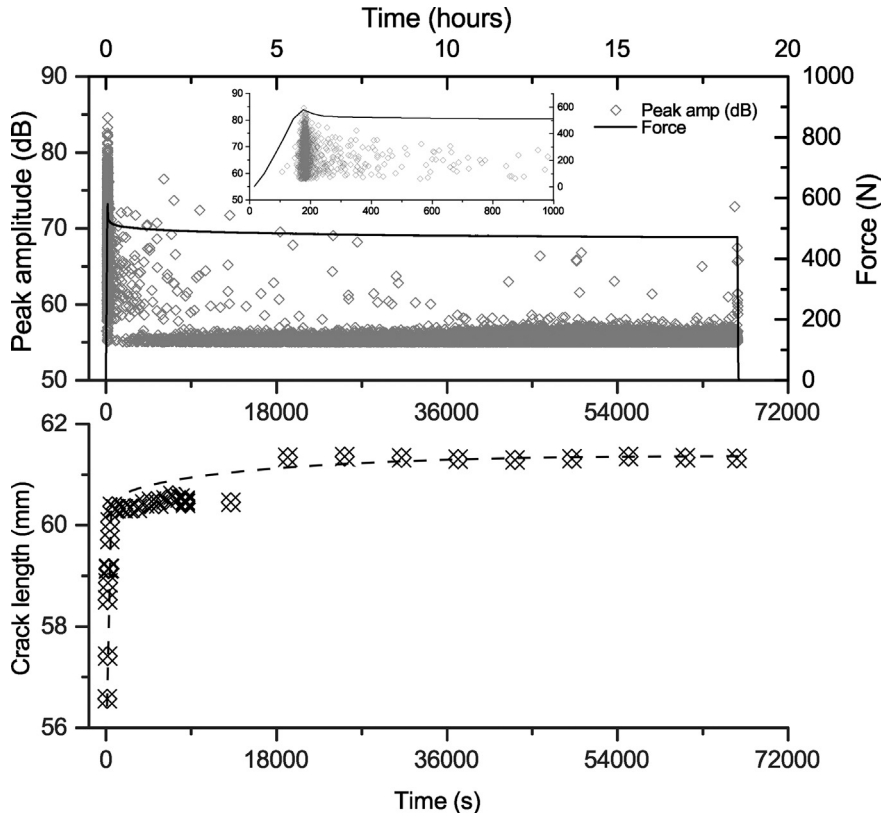


Fig. 9. Force, crack length and peak amplitude of the AE signal for experiment AE003-QS3. The load case was 1 mm/min applied displacement until the peak in the force, then the displacement was held constant. The inset figure shows a detailed view of the time period surrounding the maximum force. The force peaks at 580 N and decays asymptotically. During the last 8960 s the force is constant at 471.56 N (load cell resolution: approximately 0.3 N). In order to prevent problems rendering the graph for publication, the data is filtered to only show 1 out of every 10 hits with a peak amplitude under 58 dB (selected based on the 58 dB signal not being associated with fatigue crack growth in the previous tests). For the full data see [39]. The dashed lines are thought to give a closer approximation to the actual crack growth behaviour than the measured data points, due to the issues discussed in Fig. 8.

Thus one option to determine the SERR CG threshold is to take the time at which the first AE hit with a peak amplitude > 58 dB was measured. The SERR then follows by applying Eq. (2) to the corresponding force and displacement values.

Another option is to assume that crack growth only occurs together with the main cluster of signals surrounding the force peak (e.g. the area between the dotted lines in the right panel of Fig. 7) and that any lone signals detected before this time are some form of noise. In that case the CG threshold would be determined using the force and displacement values corresponding with the start of the main cluster.

Table 2 shows the CG threshold SERR, G_{th} , for both options. Apart from the tests shown and discussed above, this table also shows

Table 2

CG threshold SERR values measured during the quasi-static test. Values are shown for three cases: using the first AE signal with a peak amplitude over 58 dB, using the first AE signal with a peak amplitude over 62 dB, or using the left edge of the main cluster of signals. Note that for specimen AE001 the AE threshold value was 62 dB, so no signals with a peak amplitude < 62 dB were recorded. This explains why the G_{th} values for the AE001 tests are the same for the first two columns. The G_{Ic} value determined using the maximum force criterion, is also shown.

Experiment	G_{th} (N/mm)	G_{th} (N/mm)	G_{th} (N/mm)	G_{Ic} (N/mm)
	1st hit > 58 dB	1st hit > 62 dB	Main cluster	Maximum force criterion (ASTM D3433)
AE001-QS3	0.6928	0.6928	0.6928	N/A
AE001-QS4	0.7427	0.7427	0.8816	1.759
AE001-QS5	0.4047	0.4047	0.8978	1.314
AE003-QS2	0.2877	0.8814	0.8814	N/A
AE003-QS3	0.5331	0.8294	1.223	1.530
Mean	0.532	0.7102	0.915	1.534
Standard deviation	0.171 (32%)	0.1662 (23%)	0.171 (19%)	0.182 (12%)

results for experiment AE001-QS4. In that experiment the displacement was increased by 1 mm/min while the crack was allowed to grow to a length of approximately 105 mm. For the tests conducted on specimen AE001 the acoustic emission threshold was set to 62 dB, so any signals with a peak amplitude between 58 and 62 dB were not recorded. To investigate the effect of this on the measured CG threshold value, the CG threshold was also determined for the AE003 experiments using the first hit with a peak amplitude greater than 62 dB as the criterion.

Unsurprisingly, using the 1st hit > 58 dB criterion results in a lower mean G_{th} value. As can be seen from the AE003 results, increasing the peak amplitude value for CG threshold from 58 dB to 62 dB increases the determined G_{th} value. This suggests that the AE threshold setting of 62 dB used for specimen AE001 was too high to record all the relevant signals. However, in order to say which criterion is more appropriate to use, more research will need to be done in order to correlate the characteristics of the received signal to the physical processes occurring in the material.

What can be said is that crack growth occurs well before the force reaches a maximum. Therefore it seems that the onset G_{IC} value found when using the procedure given in ASTM standard D3433-99 [43] is larger than the SERR value at which crack growth physically starts, as can also be seen in Table 2. The same is likely true for the procedure given in ASTM standard D5528 [40]. This is also suggested by the results of Nikbakht et al. [45] who performed DCB tests on glass fibre reinforced polymer (GFRP) specimens with different fibre orientations. They also detected acoustic emissions well before the critical points identified by the ASTM standard, implying damage initiation for $G < G_{IC}$.

5. Results & discussion - fatigue loading

This section discusses the results of the fatigue tests. A number of different fatigue tests were performed in order to get a better understanding of the effect of crack length, maximum load, and load ratio. In order to ensure sufficient temporal resolution most tests were conducted with a displacement rate of 1 mm/min. However, a number of experiments were also conducted where fatigue cycles were applied with a frequency of 5 Hz, in order to investigate frequency effects. Due to space constraints the most relevant results are discussed here; the full data can be found online [39].

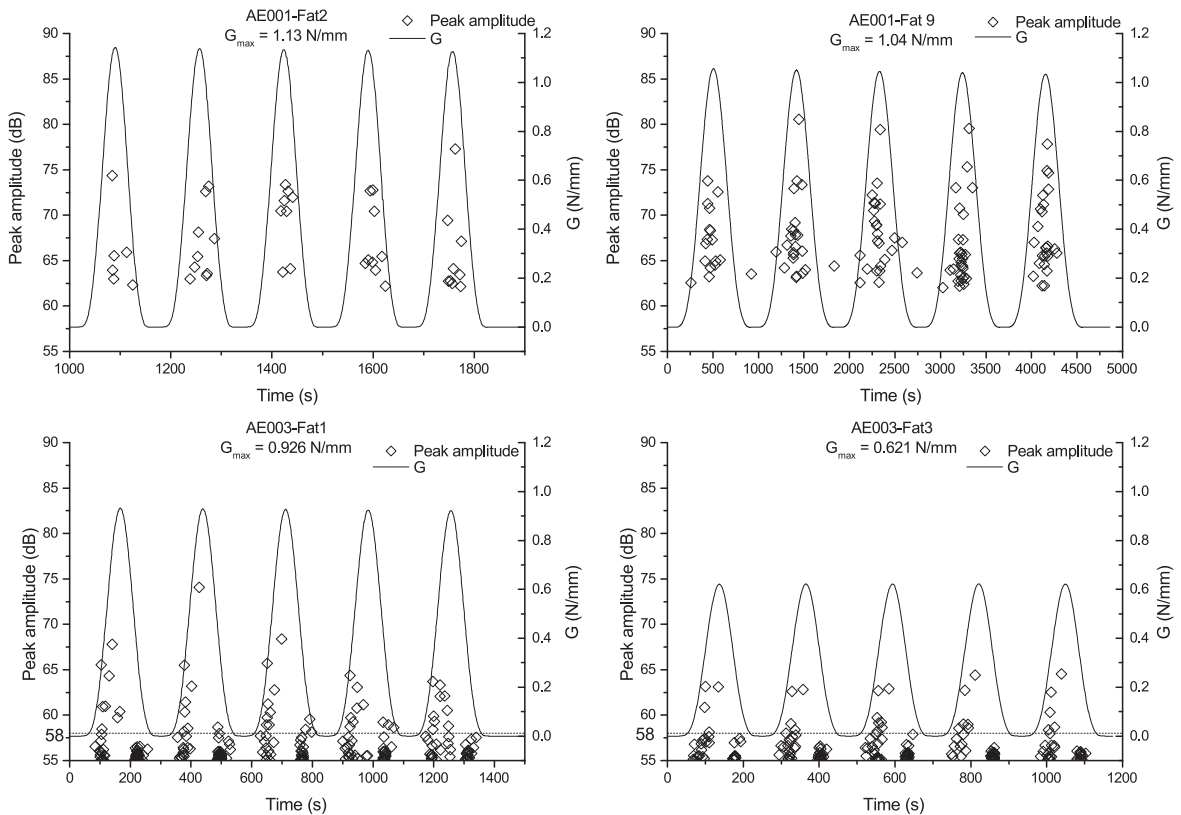


Fig. 10. SERR and peak amplitude of AE signals for the fatigue tests at $R = 0$. For experiment AE001-Fat2 the crack length was on the order of 45 mm, whereas for AE001-Fat9 it was on the order of 108 mm. Experiments AE003-Fat1 and AE003-Fat3 differ in the applied G_{max} . For specimen AE001 the AE threshold was 62 dB, for specimen AE003 it was 55 dB.

5.1. $R = 0$

The results for the fatigue tests with $R = 0$ are shown in Fig. 10. In each fatigue cycle there are a number of hits. For specimen AE001 the hits occur both during the loading and the unloading portion of the fatigue cycle. For specimen AE003 there are clusters of hits with an amplitude between 55 and 58 dB during both loading and unloading, whereas the hits with an amplitude greater than 58 dB occur only during the loading portion of the cycle. The peak amplitude of the AE signals for experiment AE003-Fat3 is noticeably lower than for AE003-Fat1, where the peak amplitude in turn is lower than for AE001-Fat2 and AE001-Fat9.

During the quasi-static tests it was seen that hits with a peak amplitude < 58 dB did not produce visible crack growth. It can of course not be ruled out that these signals correspond to an amount of crack growth that was too small to be detected with the set-up used. However these clusters of low amplitude hits (i.e. < 58 dB) occurred only during the low load portion of the fatigue cycle. Therefore it is thought that they correspond to some kind of friction or contact phenomenon during the opening and closing of the crack tip, rather than crack growth.

The clustering of the AE hits implies that fatigue crack growth only occurs during a portion of the cycle, where the G is above some CG threshold value. This aspect will be discussed below. Another notable feature is the location of the signal with the highest peak amplitude value: for experiment AE003-Fat1 this was on average for a SERR value within 80% of G_{max} . For the other experiments it was even within $>90\%$ of G_{max} . However it should be noted that this signal only represented on the order of 10–20% of the total energy received during the cycle by the transducer. So although the strongest signal is emitted close to G_{max} , this does not necessarily mean that most of the crack growth occurs there.

5.2. $R = 0.5$

The results for the fatigue tests with $R = 0.5$ are shown in Fig. 11. For specimen AE001 the results look quite similar to the results for $R = 0$. Again the AE signals occur for a narrow band of G values, indicating the presence of a CG threshold value for crack growth. The peak amplitude values reached for $R = 0.5$ and $R = 0$ are quite similar. The maximum AE signal in terms of energy content was again emitted within $>90\%$ (in fact $>97\%$ on average) of G_{max} .

For the AE003 experiments the case is quite different however. For experiment AE003-Fat2 only three cycles had signals with a

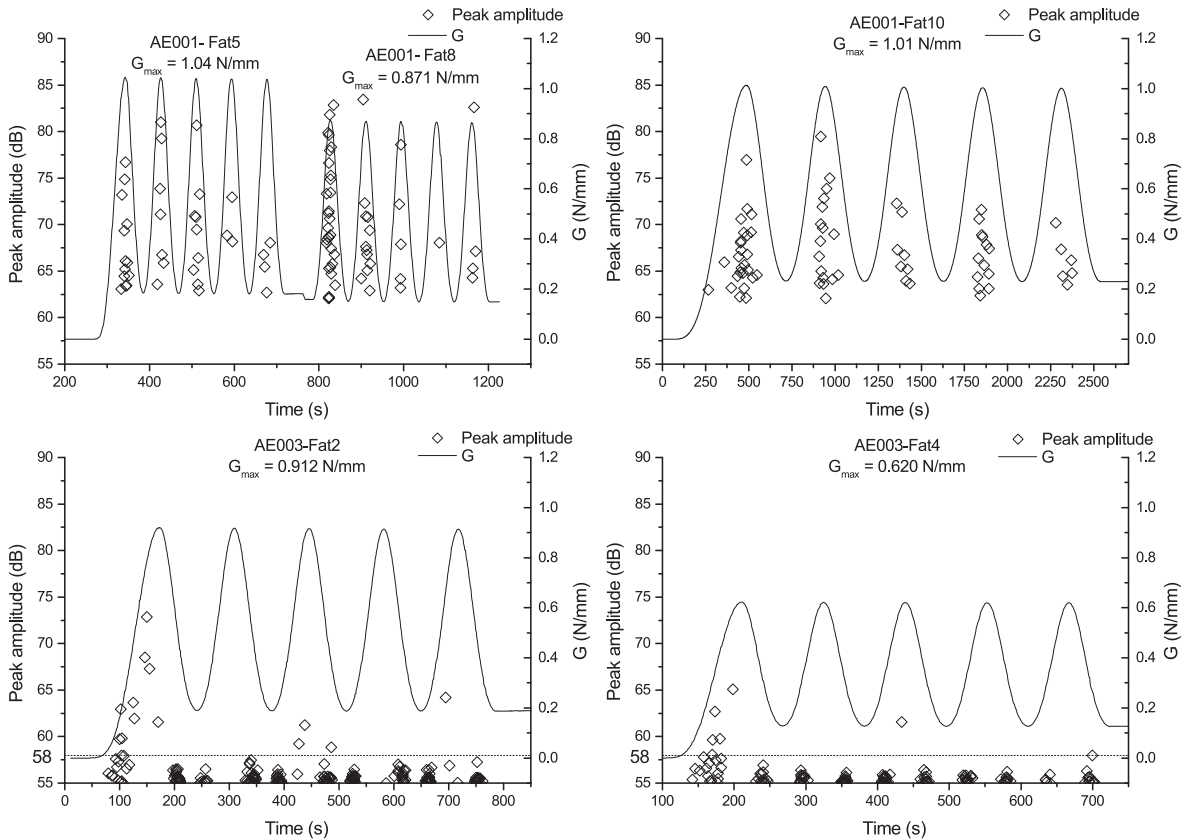


Fig. 11. SERR and peak amplitude of AE signals for the fatigue tests at $R = 0.5$. For experiments AE001-Fat5 and AE001-Fat8 the crack length was on the order of 45 mm and these experiments are therefore shown in the same panel. For experiment AE001-Fat10 the crack length was much longer: on the order of 108 mm. For specimen AE001 the AE threshold was 62 dB, for specimen AE003 it was 55 dB.

peak amplitude > 58 dB; for experiment AE003-Fat4 this was only true for two out of the five cycles. For both of these experiments there were more hits, and with a higher amplitude, during the first load cycle. During the first cycle the specimen was loaded from a minimum value of $G \approx 0$, rather than from G_{min} . Exactly why this should result in more hits is unclear however.

A point of similarity with the AE001 results is that for the cycles with a signal with a peak amplitude > 58 dB the signal with the greatest energy content occurred within > 90% of G_{max} . However for some reason specimen AE003 shows a far greater sensitivity to R-ratio.

Since the G_{max} used in the $R = 0$ and the $R = 0.5$ experiments was kept more or less constant per specimen, any R-ratio effects must be caused by the increase in minimum load. In absolute terms, during the AE003 experiments the change in minimum load was smaller than for the AE001 experiments, so on that basis one would expect a greater effect of R-ratio for specimen AE001. The opposite appears to be the case however.

5.3. CG threshold values

During the fatigue tests, signals were not emitted during the entire fatigue cycle. Thus by finding the lowest G value associated with an acoustic emission signal a crack growth threshold value can be obtained. As before, the signal with a peak amplitude greater than 58 dB was selected as the criterion for the CG threshold. In other words, the definition of the CG threshold SERR G_{th} in this section is ‘the lowest G value corresponding to an AE signal with a peak amplitude greater than 58 dB’.

The CG threshold values obtained for all fatigue experiments with a low loading rate are shown in Fig. 12. The values shown in this figure are the mean values for the set of cycles in each experiment. The scatter is quite large, as there was quite some variation from cycle to cycle in the G_{th} .

For specimen AE001 the AE threshold was set to 62 dB, whereas for specimen AE003 an AE threshold of 55 dB was used. Therefore, signals with a peak amplitude between 58 and 62 dB were not recorded for specimen AE001. To investigate the effect of this on the determined G_{th} values, Fig. 12 shows the G_{th} values determined for specimen AE003 using either 58 dB peak amplitude (left panel) or 62 dB peak amplitude (right panel) as the CG threshold criterion.

In general taking 62 dB as the criterion for CG threshold increases the found CG threshold values for specimen AE003 somewhat. However, for the $R = 0.5$ experiments (AE003-Fat2 and AE003-Fat4) there were a number of cycles where there were signals with an amplitude > 58 dB, but no signals with an amplitude > 62 dB. This means that when using 58 dB as a criterion, the mean CG threshold value was based on more cycles than when using the 62 dB criterion. As a result the mean CG threshold value when using 62 dB is lower, even though for the individual cycles where there were signals with an amplitude > 62 dB the CG threshold values increased. Even when using the 62 dB criterion the CG threshold values found for specimen AE003 were much lower than for

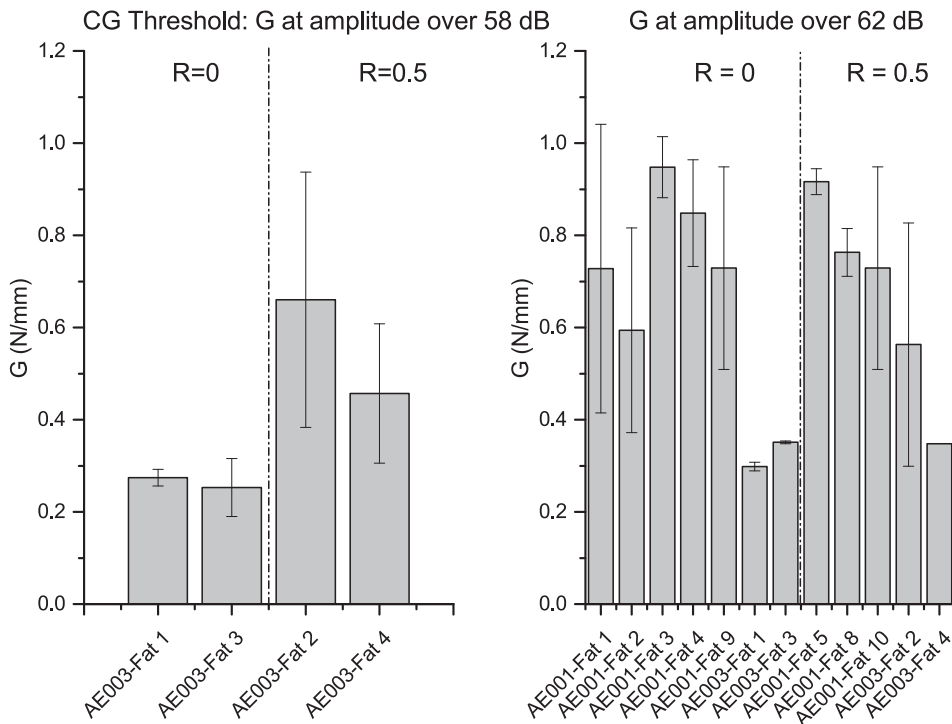


Fig. 12. Mean CG threshold values for each fatigue experiment. The error-bars show the standard deviation. The CG threshold was determined by finding the lowest G value corresponding to an AE signal with a peak amplitude greater than 58 dB (left panel) or 62 dB (right panel). Each fatigue experiment represents a set of 5 cycles. Note that for specimen AE001 the AE threshold level was set to 62 dB and thus results are only shown for the 62 dB criterion. For experiment AE003-Fat4 only 1 signal with a peak amplitude > 62 dB was detected during the entire run of 5 cycles. This explains the lack of an error-bar for this specimen.

specimen AE001, so the change in AE threshold is not sufficient to explain the observed differences between the specimens.

A possible explanation is the use of Eq. (2) to determine the SERR. If rather than using Eq. (2) a compliance calibration method is used [40], then a different calibration parameter is usually found for each specimen. Using the individually determined calibration parameters can sometimes explain the difference in measured G values between specimens [46]. This was tried for the two specimens discussed here, but was not sufficient to explain the difference in measured CG threshold values.

Another possible explanation is the crack tip condition created by the previous experiment. Experiments AE001-Fat1-5 followed experiment AE001-QS3, where the displacement was held constant for 79 min. Experiments AE001-Fat8-10 followed experiment AE001-QS5, where the displacement was held constant for 30 min. On the other hand the fatigue experiments on specimen AE003 followed experiment AE003-QS3, where the displacement was held constant for 18.5 h.

Recently Khan et al. [47] showed that for mode I fatigue in FRPs damage is created in a process zone ahead of the main delamination tip. Thus it is possible that during the long hold time of experiment AE003-QS3 damage was created ahead of the crack tip. This might make it easier for the fatigue crack to propagate in the subsequent experiments, corresponding to a lower CG threshold value. This matches with the observation that the peak amplitudes for the AE003 fatigue experiments were lower than for the AE001 experiments, suggesting that the crack growth events involved less energy. Of course the possibility that crack growth was simply slower in specimen AE003 due to material and/or specimen variability also remains a possible explanation.

A final observation from Fig. 12 is that for specimen AE003 an increase in R -ratio appears to correlate with an increase in G_{th} . However, for specimen AE001 no such R -ratio effect can be clearly identified, so further investigation is necessary to determine whether the R -ratio affects the CG threshold.

It is interesting to compare the measured fatigue CG thresholds to the CG thresholds previously determined during the quasi-static loading experiments. This comparison is shown in Fig. 13. Both the fatigue and quasi-static CG thresholds are shown for each specimen individually. Although the scatter is quite large for both the fatigue and the quasi-static values, it can be seen that the fatigue and quasi-static values seem to match. From the data presented in [41] a G_{max} of 0.4 N/mm^2 corresponds to roughly 10^{-5} mm/cycle crack growth rate, so the CG thresholds for specimen AE003 identified in Fig. 13 appear to be in the region in which the fatigue threshold would be expected (also taking into account the rough method of determining G used in this research, as discussed in Section 3.5).

Quasi-static crack growth is usually associated with G_c . One of the unanswered questions regarding fatigue crack growth is why it can occur even if $G_{max} < G_c$. As discussed above, this research shows that crack growth already occurs for $G < G_c$ even in the quasi-static case. Fig. 13 suggests that the CG threshold value for crack growth in fatigue and quasi-static growth is in fact the same. A similar conclusion was reported by Amacher et al. [48], who found that in a carbon fibre reinforced polymer (CFRP) the fatigue limit seemed to match the load at which damage initiation was detected by acoustic emission. This offers the tantalising possibility that the fatigue CG threshold value could be determined by performing a quasi-static test, rather than a fatigue test, which would represent enormous time-savings.

However first more knowledge is required on how to interpret the AE signals so that the proper CG threshold criterion can be established. Furthermore it should be determined whether crack-growth can occur while emitting signals that are indistinguishable from noise, as this possibility cannot be ruled out based on the current experiments.

5.4. Fatigue at 5 Hz

To investigate the effect of load frequency on the crack growth behaviour, a number of fatigue experiments were conducted with cycles applied at 5 Hz. Fig. 14 shows the results for experiment AE001-Fat7 ($R = 0.5$), which apart from the frequency/load rate (5 Hz vs 1 mm/min) had the same applied displacement cycle as experiments AE001-Fat5 and AE001-Fat8 (Fig. 11, top left panel).

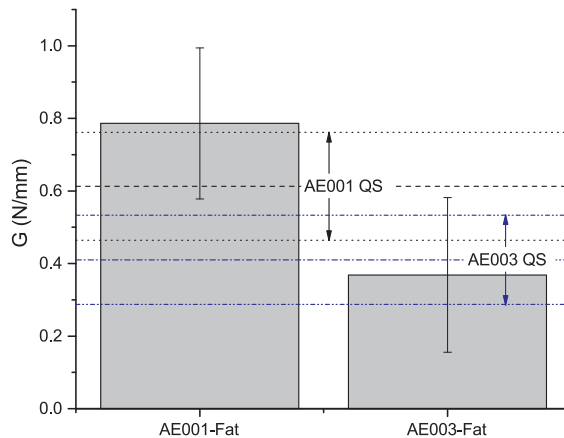


Fig. 13. Comparison between the fatigue and quasi-static CG thresholds, showing the values for each specimen individually. The vertical bars show the fatigue CG threshold value, using 58 dB peak amplitude as the criterion. The error bars represent 1 standard deviation. Similarly the horizontal lines show the mean value \pm 1 standard deviation of the quasi-static CG threshold (see also Table 2).

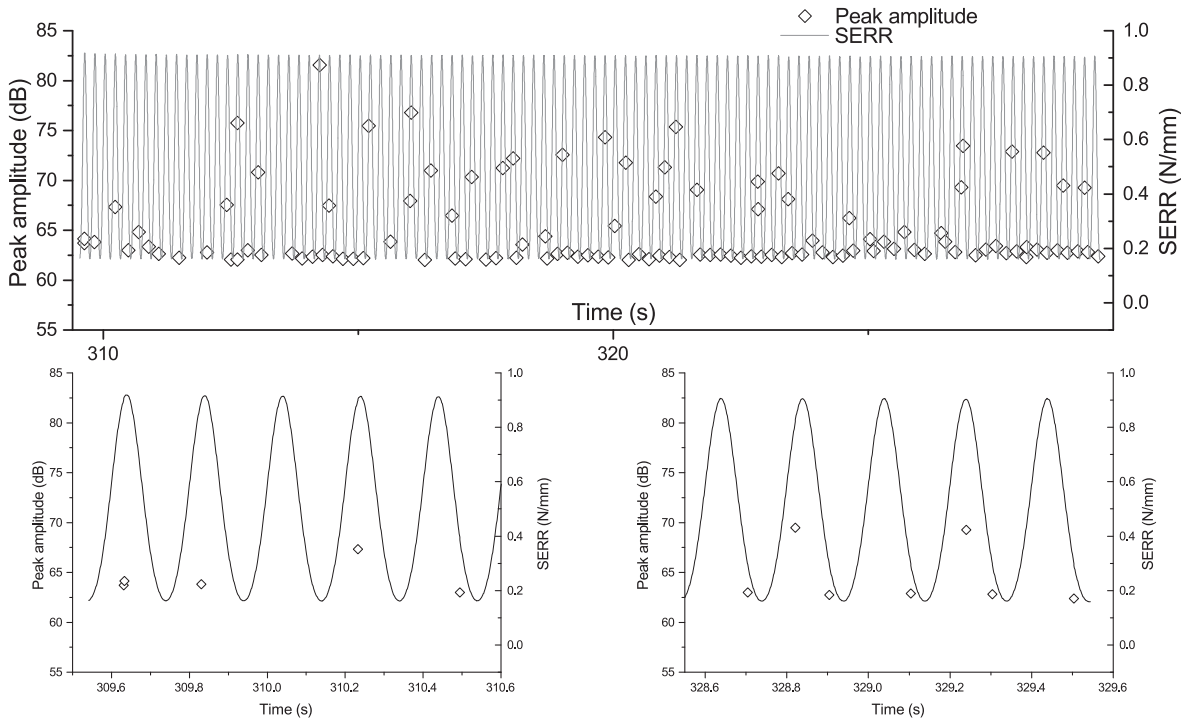


Fig. 14. Peak amplitude and SERR values for experiment AE001-Fat7. The lower figures show the first and last 5 load cycles. AE detection threshold was 62 dB.

Fig. 14 shows the entire run of 100 cycles, as well as the first 5 and last 5 cycles in greater detail.

The most obvious difference between AE001-Fat7 (5 Hz) and AE001-Fat5 (1 mm/min) is in the number of hits recorded per load cycle. During the low-rate experiments AE001-Fat5 and AE001-Fat8 (1 mm/min) many hits were recorded during each cycle, whereas at 5 Hz (AE001-Fat7) in general only one hit was recorded per cycle. For AE001-Fat7 (5 Hz) most of the hits have a low

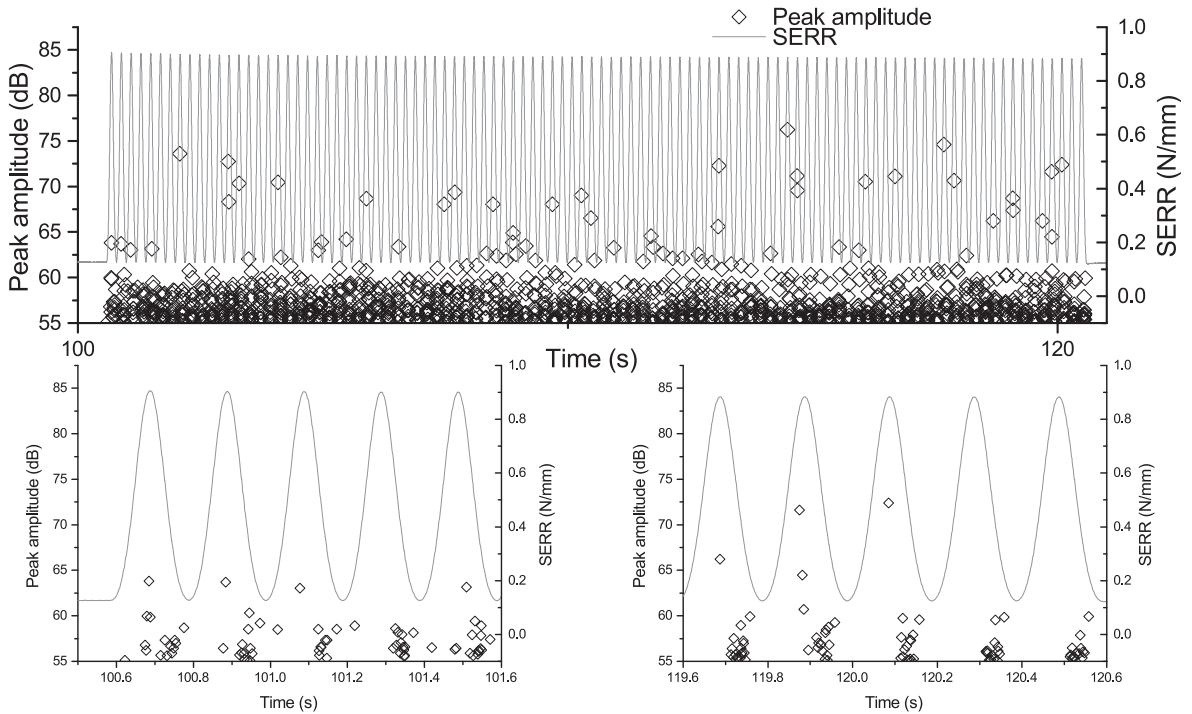


Fig. 15. Peak amplitude and SERR values for experiment AE003-Fat5. The lower figures show the first and last 5 load cycles. AE detection threshold was 55 dB.

amplitude, only just above the AE threshold. At seemingly random intervals a higher amplitude hit was detected.

Overall the AE pattern somewhat resembles what was seen in the long duration quasi-static tests: a base-line of low amplitude hits, with occasional high amplitude hits above that. Since these fatigue tests were performed under displacement control there was in both cases an initial input of energy that was depleted over the course of the test, with crack growth stopping as the energy was depleted. An important difference is that in the fatigue test a portion of this initial energy input was continuously cycled into and out of the specimen in the form of cyclic work applied by the fatigue machine. However these results suggest that it may be possible to predict the total amount of crack growth under displacement control by performing a long duration quasi-static test, which could potentially be shorter than a fatigue test that needs to reach a high number of cycles.

The results of experiment AE003-Fat5 (5 Hz, $R = 0.42$) are shown in Fig. 15. As with the low rate fatigue experiments the lower AE detection threshold here resulted in the detection of a cluster of low amplitude hits near the minimum of each load cycle. However, unlike in the low rate fatigue experiments the clusters were here only detected during unloading. The amplitude was also higher during the 5 Hz experiment. This matches the hypothesis that these clusters are associated with phenomena related to crack closure, as the higher displacement rate means crack closure will occur more forcefully.

Apart from the low amplitude clusters (which were below the 62 dB AE threshold used during AE001-Fat7 (5 Hz, $R = 0.5$)) the pattern of acoustic emission matches that seen during the 5 Hz test on specimen AE001 (AE001-Fat7).

The results of experiment AE003-Fat6 (5 Hz, $R = 0$) are shown in Fig. 16. The applied load for this experiment was the same as for AE003-Fat1 (1 mm/min, $R = 0$, Fig. 10, top right panel). Again clusters of hits are seen near the minimum load, and again they have a higher amplitude than the hits in the clusters seen during the low-rate fatigue experiments. However, unlike what was seen during experiment AE003-Fat5 (5 Hz, $R = 0.42$), the clusters here are present for both loading and unloading. The pattern here is interesting: the clusters occur near the minimum load, but no hits are detected during the time actually spent at the minimum. Similarly no hits are detected for the part of the cycle where the load is high. This provides further evidence for the hypothesis that these signals are emitted by crack opening/ closing phenomena and not by actual crack growth.

Over the entire length of the test the distribution of acoustic signals is similar to that seen on the other 5 Hz tests, with the difference that here a signal with a peak amplitude of 70–75 dB was emitted nearly every cycle, especially in the second half of the test.

Taken together the 5 Hz fatigue results shown here strongly suggest that the crack growth rate is not constant during each cycle. In most analyses crack growth is assumed to occur with a certain crack growth rate da/dN that is a continuous function of cycle number N . However, the results presented in this section imply that crack growth does not occur every cycle. Furthermore, if the peak amplitude is correlated to the amount of crack growth (as seems reasonable), the crack growth rate is also not a continuous function of N . Rather, crack growth seems to occur in a far more incremental manner, with the crack front advancing in discrete jumps.

As with the low-rate fatigue experiments, CG threshold values could be determined for each load cycle, by finding the lowest G value for which an AE signal with a peak amplitude over a certain value was detected. Fig. 17 shows the results using either 58 dB or 62 dB peak amplitude as the CG threshold criterion. It also shows a comparison with the CG threshold values found for the low-rate

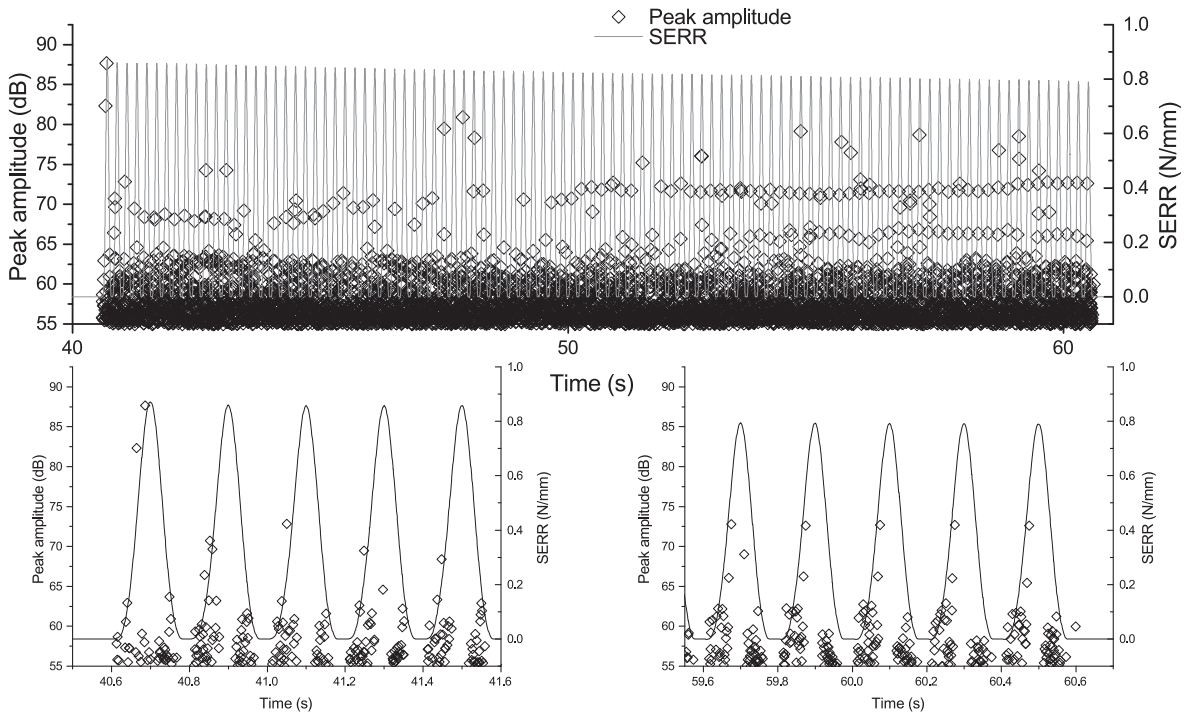


Fig. 16. Peak amplitude and SERR values for experiment AE003-Fat6. The lower figures show the first and last 5 load cycles. AE detection threshold was 55 dB.

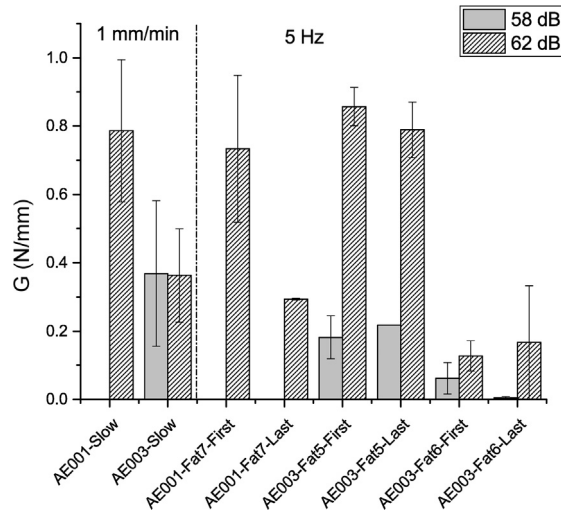


Fig. 17. Comparison of the measured crack growth thresholds for the low rate fatigue and the 5 Hz fatigue cycles, using either 58 dB or 62 dB as the CG threshold criterion. For AE001 the AE threshold setting was 62 dB and so there is no difference between the 58 and the 62 dB criterion for those experiments. CG threshold values were determined for the first and last 5 cycles for each 5 Hz experiment.

fatigue experiments.

Unsurprisingly taking 62 dB as the CG threshold criterion results in a higher value for the measured G CG threshold. For the 5 Hz experiments this effect is much more pronounced than for the low-rate experiments (compare Fig. 12). A possible explanation is the higher amplitude of the clusters of hits detected near to the cycle minima. For the 5 Hz experiments some of these signals reached a peak amplitude greater than 58 dB, whereas during the low-rate fatigue these signals had a lower maximum peak amplitude. This suggests that if peak amplitude is being used as a criterion to filter actual crack growth signals from other signals, the peak amplitude value to be used should depend on the loading frequency. Using a different feature of the received signals to discriminate between crack growth and other phenomena may therefore be preferred.

Further interesting results from Fig. 17 are that there is a difference between the CG thresholds measured at the beginning and at the end of the test. There also is a clear effect of frequency on the CG threshold. The difference in CG threshold values at the beginning and end of the test may be caused by formation of a damage zone. The frequency effect may be related to strain-rate effects. However, further research is needed to investigate these hypotheses.

6. Conclusions

The acoustic emission technique was used to investigate both quasi-static crack growth and fatigue crack growth behaviour during a single fatigue cycle. Although many details still need further investigation, it is clear that this technique can provide more insight into crack growth behaviour. Due to the small amount of crack growth that typically occurs during a single cycle, optical systems cannot be used to detect this. Acoustic emission provides a way of solving this issue, allowing one to pin-point exactly during which part of the fatigue cycle crack growth takes place.

Under quasi-static load, crack growth occurs before non-linearity of the force-displacement curve, and before the force reaches a maximum. This means that the G_{Ic} value that is found using current quasi-static test protocols should not be interpreted as the minimum G value at which crack growth can occur.

In fatigue, it appears that the crack can grow both during the loading and during the unloading phase of the load cycle. Crack growth does not just occur at maximum load, but also does not occur near to the minimum load, making the physical relevance of G_{max} and $\Delta G = G_{max} - G_{min}$ as similitude parameters for fatigue crack growth unclear. Crack growth appears to occur during the part of the load cycle that is above a certain CG threshold value. This CG threshold value is not necessarily a material property, but may also depend on the load history and perhaps test frequency. The CG threshold in fatigue appears to match the value of G at which crack growth starts under quasi-static loading, but given the large scatter in the data this could not be entirely confirmed.

In order to confirm the results mentioned above future research should focus on establishing a link between the physical mechanisms of crack growth and the received acoustic emission signals. This will allow better filtering of the received signals in order to determine which signals are relevant to crack growth. It will also provide physical justification for the criteria used to determine the CG threshold SERR values. In the current research, an optical technique was used to attempt to relate the acoustic emission signals to crack growth. However, this technique suffers from a number of limitations. The expected crack growth in a single cycle is too small to be reliably detected. Furthermore, only crack growth on the surface of the specimen can be monitored, and it could not be investigated whether there was a process zone ahead of the crack tip - which may affect the crack growth and any CG thresholds.

One possibility to improve this would be to combine acoustic emission with (micro)-radiographic techniques, as recently done in [49], although that may be more applicable for cracks in FRPs than in metal-to-metal adhesive bonds. In-situ testing in an SEM, such

as in the recent work of Khan et al. [47] may also provide useful insights.

In addition sources of noise should be understood and eliminated so that even faint crack growth signals can be detected, in order to be sure that all crack growth is captured using the AE measurement technique.

In metals, quite some success has been achieved in relating acoustic emission signals to specific physical processes [50]. Various signal processing techniques (e.g. [51]) in combination with the non-destructive inspection techniques mentioned above, may help achieve similar results for adhesive bonds and composites.

With these improvements acoustic emission can prove a valuable tool for gaining more insight into the physical process of fatigue crack growth, and help determine which features of a fatigue cycle are relevant for predicting crack growth. This will allow better validation of micro-mechanical models of fatigue crack growth and result in a more complete scientific understanding of this phenomenon.

Acknowledgements

The authors express their gratitude to Dr. D. Bürger for supplying the specimens used in this research. J.A. Pascoe thanks the Netherlands Organisation for Scientific Research (NWO) for supporting his work financially through a grant from the Mosaic programme, under Grant No. 017.009.005.

Appendix A. Supplementary material

Supplementary data associated with this article can be found, in the online version, at <http://dx.doi.org/10.1016/j.engfracmech.2018.03.012>.

References

- [1] Paris P, Gomez M, Anderson W. A rational analytic theory of fatigue. *Trend Eng* 1961;13:9–14.
- [2] Paris P. The fracture mechanics approach to fatigue. In: 10th Sagamore army materials research conference. Syracuse University Press; 1964. p. 107–32.
- [3] Paris P, Erdogan F. A critical analysis of crack propagation laws. *J Basic Eng* 1963;85(4):528–33.
- [4] Roderick G, Everett R, Crews Jr J. Debond propagation in composite reinforced metals, Tech. Rep. NASA TM X-71948. NASA; 1974.
- [5] Mostovoy S, Ripling E. Flaw tolerance of a number of commercial and experimental adhesives, polymer science and technology 9B. New York: Plenum Press; 1975. p. 513–62.
- [6] Irwin GR. Analysis of stresses and strains near the end of a crack traversing a plate. *ASME J Appl Mech* 1957;24:361–4.
- [7] Xie Y, Koslowski M. Numerical simulations of inter-laminar fracture in particle-toughened carbon fiber reinforced composites. *Composites Part A* 2017;92:62–9.
- [8] Li S, Wang G. On damage theory of a cohesive medium. *Int J Eng Sci* 2004;42(8–9):861–85.
- [9] Wang G, Li SF. A penny-shaped cohesive crack model for material damage. *Theoret Appl Fract Mech* 2004;42(3):303–16.
- [10] Brighenti R, Carpinteri A, Scorza D. Micromechanical crack growth-based fatigue damage in fibrous composites. *Int J Fatigue* 2016;82(Part 1):98–109.
- [11] Hojo M, Tanaka K, Gustafson CG, Hayashi R. Effect of stress ratio on near-threshold propagation of delamination fatigue cracks in unidirectional CFRP. *Compos Sci Technol* 1987;29(4):273–92.
- [12] Allegri G, Wisnom MR, Hallett SR. A new semi-empirical law for variable stress-ratio and mixed-mode fatigue delamination growth. *Composites Part A* 2013;48(0):192–200.
- [13] Jones R, Kinloch AJ, Hu W. Cyclic-fatigue crack growth in composite and adhesively-bonded structures: the FAA slow crack growth approach to certification and the problem of similitude. *Int J Fatigue* 2016;88:10–8.
- [14] Andersons J, Hojo M, Ochiai S. Empirical model for stress ratio effect on fatigue delamination growth rate in composite laminates. *Int J Fatigue* 2004;26(6):597–604.
- [15] Kaiser J. Erkenntnisse und folgerungen aus der messung von geräuschen bei zugbeanspruchung von metallischen werkstoffen. *Archiv für das Eisenhüttenwesen* 1953;24(1/2):43–5.
- [16] Tang J, Souza S, Mares C, Gan T-H. An experimental study of acoustic emission methodology for in service condition monitoring of wind turbine blades. *Renew Energy* 2016;99:170–9.
- [17] Saedifar M, Fotouhi M, Ahmadi Najafabadi M, Hosseini Toudeshky H, Minak G. Prediction of quasi-static delamination onset and growth in laminated composites by acoustic emission. *Compos Part B: Eng* 2016;85:113–22.
- [18] Crivelli D, Guagliano M, Eaton M, Pearson M, Al-Jumaili S, Holford K, et al. Localisation and identification of fatigue matrix cracking and delamination in a carbon fibre panel by acoustic emission. *Compos Part B: Eng* 2015;74:1–12.
- [19] Okafor AC, Singh N, Singh N, Oguejiofor BN. Acoustic emission detection and prediction of fatigue crack propagation in composite patch repairs using neural network. *J Thermoplast Compos Mater* 2017;30(1):3–29.
- [20] Dzenis YA. Cycle-based analysis of damage and failure in advanced composites under fatigue. *Int J Fatigue* 2003;25(6):499–510.
- [21] Brunner A, Nordstrom R, Flüeler P. A study of acoustic emission-rate behavior in glass fiber-reinforced plastics. *J Acoust Emission* 1995;13(3–4):67–77.
- [22] Pascoe JA, Alderliesten RC, Benedictus R. Methods for the prediction of fatigue delamination growth in composites and adhesive bonds - a critical review. *Eng Fract Mech* 2013;112–113:72–96.
- [23] Griffith AA. The phenomena of rupture and flow in solids. *Philos Trans R Soc Lond Ser A. Contain Pap Math Phys Charact* 1921;221:163–98.
- [24] Weertman J. Rate of growth of fatigue cracks as calculated from the theory of infinitesimal dislocations distributed on a plane. In: Yokobori T, Kawasaki T, Swedlow J, editors. *Proceedings of the first international conference on fracture*. Japanese Society for Strength and Fracture of Materials; 1965. p. 153–64.
- [25] Weertman J. Theory of fatigue crack growth based on a BCS crack theory with work hardening. *Int J Fract* 1973;9(2):125–31.
- [26] Chudnovsky A, Moet A. Thermodynamics of translational crack layer propagation. *J Mater Sci* 1985;20:630–5.
- [27] Chudnovsky A, Moet A. On the law of fatigue crack layer propagation in polymers. *Polym Eng Sci* 1982;22(15):922–7.
- [28] Ranganathan N, Chalou F, Meo S. Some aspects of the energy based approach to fatigue crack propagation. *Int J Fatigue* 2008;30(10–11):1921–9.
- [29] Ranganathan N. The energy based approach to fatigue. *Adv Mater Res* 2014;891–892:821–6. [11th International Fatigue Congress].
- [30] Meneghetti G. Analysis of the fatigue strength of a stainless steel based on the energy dissipation. *Int J Fatigue* 2007;29(1):81–94. <http://dx.doi.org/10.1016/j.ijfatigue.2006.02.043> <<http://www.sciencedirect.com/science/article/pii/S0142112306000764>> .
- [31] Meneghetti G, Ricotta M, Atzori B. Experimental evaluation of fatigue damage in two-stage loading tests based on the energy dissipation. *Proc Inst Mech Engin, Part C: J Mech Eng Sci* 2015;229(7):1280–91. <http://dx.doi.org/10.1177/0954406214559112>.
- [32] Pascoe JA, Alderliesten RC, Benedictus R. On the relationship between disbond growth and the release of strain energy. *Eng Fract Mech* 2015;133:1–13.
- [33] Yao L, Alderliesten RC, Zhao M, Benedictus R. Discussion on the use of the strain energy release rate for fatigue delamination characterization. *Composites Part A* 2014;66(0):65–72.

- [34] Amaral L, Yao L, Alderliesten R, Benedictus R. The relation between the strain energy release in fatigue and quasi-static crack growth. *Eng Fract Mech* 2015;145:86–97.
- [35] Atodaria DR, Putatunda SK, Mallick PK. A fatigue crack growth model for random fiber composites. *J Compos Mater* 1997;31(18):1838–55.
- [36] Allegri G, Jones MI, Wisnom MR, Hallett SR. A new semi-empirical model for stress ratio effect on mode II fatigue delamination growth. *Composites Part A* 2011;42(7):733–40.
- [37] Jones R, Pitt S, Bunner AJ, Hui D. Application of the Hartman-Schijve equation to represent mode I and mode II fatigue delamination growth in composites. *Compos Struct* 2012;94(4):1343–51.
- [38] Bürger D. Mixed-mode fatigue disbond on metallic bonded joints, Phd thesis. Delft University of Technology; 2015, doi:<http://dx.doi.org/10.4233/uuid:ec4dbcd6-052d-4009-bf9e-cdcfb4614174>.
- [39] Pascoe JA, Zarouchas D, Alderliesten RC. Acoustic emission during crack growth in FM94 epoxy; 2016, doi:<http://dx.doi.org/10.4121/uuid:8cb928b4-4dc9-4420-8adc-f1273c9fd7c5>.
- [40] ASTM Standard D 5528/ D 5528-01. Standard test method for mode I interlaminar fracture toughness of unidirectional fiber-reinforced polymer matrix composites. West Conshohocken (PA, USA): ASTM International; 2007.
- [41] Pascoe JA. Characterising fatigue crack growth in adhesive bonds, Ph.D. thesis. Delft University of Technology; 2016 < <http://repository.tudelft.nl/islandora/object/uuid%3Aebbf552a-ce98-4ab6-b9cc-0b939e12ba8b?collection=research> > .
- [42] Alderliesten RC. How proper similitude can improve our understanding of crack closure and plasticity in fatigue. *Int J Fatigue* 2016;82(Part 2):263–73.
- [43] ASTM Standard D3433-99. Standard test method for fracture strength in cleavage of adhesives in bonded metal joints. West Conshohocken (PA, USA): ASTM International; 2012.
- [44] Davidson B, Schapery R. Effect of finite width on deflection and energy release rate of an orthotropic double cantilever specimen. *J Compos Mater* 1988;22(7):640–56.
- [45] Nikbakht M, Yousefi J, Hosseini-Toudeshky H, Minak G. Delamination evaluation of composite laminates with different interface fiber orientations using acoustic emission features and micro visualization. *Compos Part B: Eng* 2017;113:185–96.
- [46] Murri GB. Evaluation of delamination onset and growth characterization methods under mode I fatigue loading. In: 27th Technical conference on American society for composites. Arlington (TX): DEStech Publications, Inc.; 2012. p. 601–20.
- [47] Khan R, Alderliesten R, Badshah S, Khattak MA, Khan MS, Benedictus R. Experimental investigation of the microscopic damage development at mode I fatigue delamination tips in carbon/epoxy laminates. *Jurnal Teknologi* 2016;78(11).
- [48] Amacher R, Cugnoli J, Botsis J, Sorensen L, Smith W, Dransfeld C. Thin ply composites: experimental characterization and modeling of size-effects. *Compos Sci Technol* 2014;101:121–32.
- [49] Brunner AJ. Correlation between acoustic emission signals and delaminations in carbon fiber-reinforced polymer-matrix composites: a new look at mode I fracture test data. *J Acoust Emission* 2016;33:S41–9.
- [50] Vinogradov A, Patlan V, Hashimoto S, Kitagawa K. Acoustic emission during cyclic deformation of ultrafine-grain copper processed by severe plastic deformation. *Philos Magaz A* 2002;82(2):317–35. <http://dx.doi.org/10.1080/01418610208239601>.
- [51] Pomponi E, Vinogradov A. A real-time approach to acoustic emission clustering. *Mech Syst Sig Process* 2013;40(2):791–804. <http://dx.doi.org/10.1016/j.ymssp.2013.03.017>. URL. < <http://www.sciencedirect.com/science/article/pii/S0888327013001179> > .